

Geophysics Open-File Report 1  
Geoscience Department  
New Mexico Tech  
Socorro, NM 87801

*Independent  
Study*

GRAVITY SURVEY IN SOUTHERN END OF ALBUQUERQUE-BELLEVUE BASIN, SOCORRO COUNTY

NEW MEXICO

BY

KRAI HUT      WONGYI WAT

INDEPENDENT STUDY PRESENTS TO DR. A. R. SANFORD

NEW MEXICO INSTITUTE OF MINING AND TECHNOLOGY, SOCORRO, NEW MEXICO

MAY 25, 1970.

## CONTENTS

ACKNOWLEDGEMENTS. . . . .	v
ABSTRACT. . . . .	vi
INTRODUCTION. . . . .	1
THEORY OF GRAVITY EXPLORATION . . . . .	4
a. Newton's law of Gravitation. . . . .	4
b. Figure of the earth. . . . .	5
c. Corrections to datum . . . . .	7
d. Surface densities. . . . .	11
e. Tidal corrections. . . . .	12
f. Gravity anomalies. . . . .	13
SURVEY PROCEDURES. . . . .	14
CALCULATION OF BOUGJER ANOMALIES. . . . .	16
a. Datum. . . . .	16
b. Elevation corrections. . . . .	16
c. Terrain correction : . . . . .	16
d. Theoretical gravity. . . . .	17
BOUGJER GRAVITY MAPS. . . . .	23
GEOLOGY OF THE GRAVITY SURVEY AREA. . . . .	27
a. Stratigraphy. . . . .	27
b. Structure. . . . .	29

INTERPRETATION. . . . .	.31
a. Qualitative interpretation . . . . .	.31
b. Quantitative interpretation. . . . .	.36
SUMMARY AND CONCLUSIONS . . . . .	.48
APPENDIX . . . . .	.49
BIBLIOGRAPHY. . . . .	.57

## LIST OF FIGURES

FIGURE 1. MAP OF THE GRAVITY SURVEY AREA. . . . .	3
FIGURE 2. THE FIGURE OF THE EARTH . . . . .	5
FIGURE 3. DIAGRAM ILLUSTRATING FREE-AIR CORRECTION. . . . .	8
FIGURE 4. DIAGRAM ILLUSTRATING BOUGUER PLATE CORRECTION . . . . .	10
FIGURE 5. DIAGRAM ILLUSTRATING TERRAIN CORRECTION . . . . .	11
FIGURE 6. GEOLOGIC MAP OF SOUTHERN END OF ALBUQUERQUE-BELLEVUE BASIN, SOCORRO COUNTY, NEW MEXICO. . . . .	19
FIGURE 7a. TOTAL BOUGUER ANOMALIES MAP . . . . .	20
FIGURE 7b. TOTAL BOUGUER ANOMALIES MAP . . . . .	21
FIGURE 8. REGIONAL BOUGUER ANOMALIES MAP. . . . .	22
FIGURE 9a. RESIDUAL ANOMALIES MAP. . . . .	25
FIGURE 9b. RESIDUAL ANOMALIES MAP. . . . .	26
FIGURE 10. GEOLOGIC SECTION USED IN GRAVITY INTERPRETATIONS. . . . .	37
FIGURE 11. 5-SIDED POLYGON OF TWO DIMENSIONAL BODY . . . . .	40
FIGURE 12. TWO DIMENSIONAL GRAVITY ANOMALIES MODEL, PROFILE AA' . . . . .	43
FIGURE 13. TWO DIMENSIONAL GRAVITY ANOMALIES MODEL, PROFILE BB' . . . . .	44
FIGURE 14. HYPOTHETICAL GEOLOGIC SECTION ALONG PROFILE AA' WITH OBSERVED AND COMPUTED GRAVITY ANOMALIES . . . . .	45
FIGURE 15. HYPOTHETICAL GEOLOGIC SECTION ALONG PROFILE BB' WITH OBSERVED AND COMPUTED GRAVITY ANOMALIES . . . . .	46
FIGURE 16. DIAGRAM FOR THE GRADIENT OF THEORETICAL GRAVITY VALUES. . . . .	49
FIGURE 17. DIAGRAM ILLUSTRATING BOUGUER PLATE CORRECTION . . . . .	50
FIGURE 18. THE DIAGRAM OF DRIFT CORRECTION . . . . .	52
FIGURE 19. GRAVITY PROFILE ACROSS THE TWO DIMENSION VERTICAL FAULT. . . . .	53

LIST OF TABLE

TABLE I.	BOUGUER GRAVITY ANOMALIES AND CORRECTIONS. . .	32
TABLE I (CONTINUED)	BOUGUER GRAVITY ANOMALIES AND CORRECTIONS. . .	33
TABLE I (CONTINUED)	BOUGUER GRAVITY ANOMALIES AND CORRECTIONS. . .	34
TABLE II	OBSERVED AND COMPUTED GRAVITY ANOMALIES. . .	42
TABLE III	DRIFT CORRECTION . . . . .	52

#### ACKNOWLEDGEMENT

The writer is grateful to Dr. Allen R. Sanford of New Mexico Institute of Mining and Technology for his valuable advices during the period of study and during the preparation of this paper. The writer also deeply appreciates to Dr. A. J. Budding of the same Institute for his help.

I am indebted to Mr. Don Adams who assisted in the field, and Mr. S. Rodphothong who did some part of the typing.

## ABSTRACT

The reduction of observed gravity anomalies are latitude, elevation terrain, and drift corrections. All of these corrections are explained in this paper. The field technique of gravity survey by Worden gravity meter and the gravity data have been shown. The depth to the base of Santa Fe formation of Tertiary age is interpreted by the calculation and construction the models of two profiles. The (computed) gravity anomalies are computed by the computer.

## INTRODUCTION

The gravity method of exploration is one of the best methods in geophysical exploration to determine the location of oil field; the geologic structures; the location of rocks, and some materials in the subsurface by means of the density of each formation, which are the only sources of gravity method.

The purpose of this paper is the study of structure of Rio Grande trough by using the gravity method and the interpretation to the depth of Santa Fe formation of Tertiary age by construction the models. The thickness of Santa Fe formation can also calculate from the vertical fault. The interpretation is under the following assumptions.

1. the geologic section of the gravity survey area is given,
2. the geologic structures are two dimensional,
3. the rock units are horizontal.

The standard model of Worden gravity meter, no. 110, which is the property of New Mexico Institute of Mining and Technology, is used in this gravity survey. About 88 gravity stations have been occupied in the gravity survey area.

The elevation of some gravity stations are known exactly, by the description of Bench Mark. The elevation of the other gravity stations are used directly from the elevation values as shown in the United States Department of Interior, Geological Survey, quadrangle maps of 7.5 minute series; this elevation values are shown only the interger values.

The gravity survey area is Bernardo, which is located at the north of Socorro city about 26 miles, and in the vicinity at about latitude



34°20' N to 34°30' N and longitude 106°30' W to 107°00' W.\*This area is in the southern end of Albuquerque-Belen basin. The Monzano and Los Pinos mountains are located on the eastern margin; and Ladron mountains are located on the western margin.

\* See Figure 1.

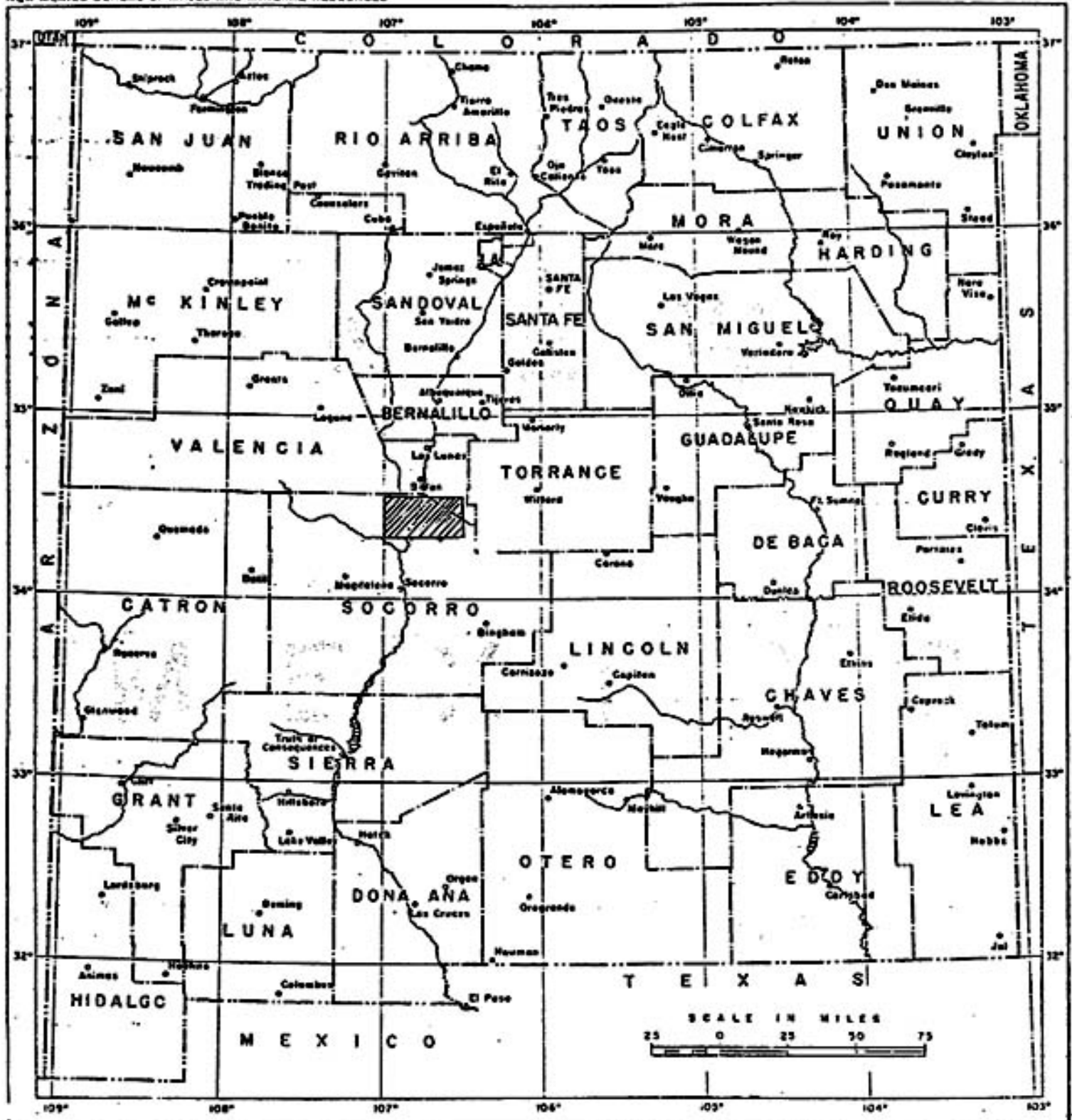


FIGURE 1. MAP OF THE GRAVITY SURVEY AREA

## THEORY OF GRAVITY EXPLORATION

### A. NEWTON'S LAW OF GRAVITATION

The object of the gravity method in geophysical exploration is the determination of structure in the subsurface by measuring the variations in gravity on the surface of the earth following Newton's Law of Gravitation. Newton's Law of Gravitation states that the forces (dynes) between the masses  $m_1$  and  $m_2$  (grams); and the distance between the masses is  $r$  (centimeters), is,

$$F = \frac{G m_1 m_2}{r^2} ,$$

where,  $F$  is the forces (dynes),

$G$  is the universal gravitation constant,

$$G = 6.670 \times 10^{-8} \text{ cm}^3/\text{gram-second}^2.$$

When the object ( $m_1$ ) moves with the acceleration  $a$ , the force is,

$$F = m_1 a,$$

and when the object ( $m_1$ ) is on the earth, the force is,

$$F = \frac{G m_1 m_e}{r_e^2} ,$$

where,  $m_e$  is the mass of the earth =  $5.983 \times 10^{27}$  grams,

$r_e$  is an average radius of the earth =  $6371.221 \times 10^5$  centimeters,

$a = g$  is the gravity value of the earth (gal or  $\text{cm}/\text{second}^2$ ).

Therefore,

$$g = a = \frac{G m_e}{r_e^2} .$$

In the geophysical exploration, the unit of acceleration or gravity

anomalies [are expressed in] MILLIGAL,

where, 1 mgal = 1 milligal =  $10^{-3}$  gal.

The average gravity values of the earth is about 980 gals, and the gravity values are varied of 978.049 to 983.221, from the equator to the poles of the earth.

### 9. FIGURE OF THE EARTH

The earth is not a perfectly sphere, but [it is] an ellipsoid. The equatorial radius of the earth is longer than the polar radius of the earth about 21 kilometers.

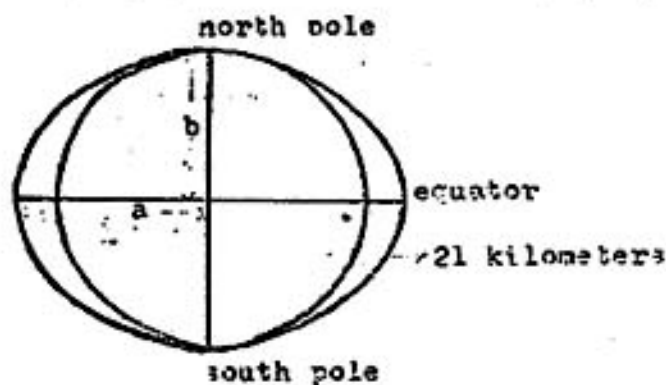


Figure 2. The figure of the earth.

As shown in figure 2,

a is the equatorial radius of the earth = 6378.388 kilometers.

b is the polar radius of the earth = 6356.912 kilometers.

I. The earth rotates around itself, [and revolves around the sun]

so the gravity values of the earth should be affected by the gravitational attractions and the centrifugal forces,

1. the gravity values effect by gravitational attractions,

$g_e$  = the gravity value of the earth at the equator,

$$= \frac{G m_e}{a^2}$$

$g_p$  = the gravity value of the earth at the pole,

$$= \frac{G m_e}{b^2}$$

because the value  $a$  is greater than the value  $b$ , so then, the value of

$g_p$  is greater than the value of  $g_e$ ,

therefore,  $g_p - g_e = 6.6$  gals,

2. the gravity values effect by centrifugal forces,

$g'_e$  = the centrifugal forces of the earth at the equator,

$$= 3.4 \text{ gals,}$$

$g'_p$  = the centrifugal forces of the earth at the pole,

$$= 0 \text{ gal.}$$

Due to the gravitational attractions and the centrifugal forces,

the gravity value of the earth at the pole is greater than the gravity value of the earth at the equator,

$$= 6.6 + 3.4 = 10 \text{ gals.}$$

II. But the equatorial radius is greater than the polar radius 21 kilometers, therefore, the gravity value of the earth at the equator, when the thickness is 21 kilometers, is,

$$= 2\pi\rho G h^2 = 4.8 \text{ gals,}$$

where,  $\rho$  = the mean density of the earth = 5.522 gram/cm<sup>3</sup>,

210 13  
Series 411  
11 4 21  
on this and  
subsequent  
pages.

$$h = 21 \text{ kilometers.}$$

Therefore, the gravity value of the earth at the pole is greater than the gravity value of the earth at the equator,

$$= 10.0 - 4.8 = 5.2 \text{ gals.}$$

### C. CORRECTION TO DATUM

The observed gravity values are affected by many factors, these factors must be corrected to the datum.

1. *Latitude Corrections*  
 1. LATITUDE CORRECTIONS --- *You need different type of heading here.*

From the figure of the earth, the gravity of the earth varied with the change of latitude from the equator to the pole.\* This gravity values are the theoretical gravity values which can be determined by the international gravity formula.

$$g_{th} = g_0 (1 + C_1 \sin^2 \phi - C_2 \sin^2 2\phi).$$

where,  $g_0$  is the gravity value of the earth at the equator,

$\phi$  is the latitude value at the gravity station.

$$c = \frac{a - b}{a}$$

$c = \frac{\text{equatorial radius of the earth} - \text{polar radius of the earth}}{\text{equatorial radius of the earth}}$

$$c = \frac{a^2 - b^2}{a^2}$$

$$C_1 = \frac{5}{2} c - c - \frac{17}{14} c,$$

\* See page 6.

$$c_2 = \alpha \left( \frac{5}{8} - \frac{1}{8} \alpha \right).$$

The international Union of Geodesy and Geophysics in 1930 used the absolute gravity value of 981.274 gals measured at Potsdam to calculate the value of  $g_{th}$ . That expression is,

$$g_{th} = 978.04900(1 + 0.005288384 \sin^2 \phi - 0.000005869 \sin^2 2\phi).$$

The calculation of the value of theoretical gravity by this way, the exact value of the latitude of every gravity station has to find out. So, this gravity survey is used the particular method for latitude corrections.\*

## II. ELEVATION CORRECTIONS

### 1. Free-air correction .

This correction assumed that the observation station had been taken in the free air at the height above datum  $h$  and no any other materials between the observation station and the <sup>center</sup> center of the earth. When the observation stations are far away from the <sup>datum</sup> center of the earth, the gravity values will be decreased. So, the free-air corrections are always positive.

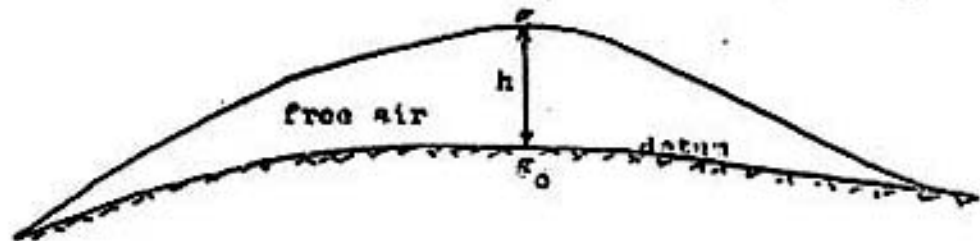


Figure 3. Diagram illustrating free-air correction .

\* See page 17.

As shown in figure 3,

$g$  is the observed gravity values at the point  $h$  above datum,

$g_0$  is the gravity values at datum,

$m_e$  is the mass of the earth =  $5.983 \times 10^{27}$  grams,

$r_e$  is the average radius of the earth, (assuming that the earth is a perfect sphere) =  $6371.221 \times 10^5$  centimeters.

Then, 
$$g_0 = \frac{G m_e}{r_e^2}$$

and, 
$$g = \frac{G m_e}{(r_e + h)^2}$$

$$g = G m_e r_e^{-2} \left(1 + \frac{h}{r_e}\right)^{-2},$$

therefore, 
$$g = g_0 \left(1 - \frac{2h}{r_e} + 3\left(\frac{h}{r_e}\right)^2 - \dots\right),$$

$h$  is very small when compare with  $r_e$ , so,  $\left(\frac{h}{r_e}\right)^2$  and higher order terms are ignored.

Therefore, the free-air corrections are,

$$g_0 - g = \frac{2 g_0 h}{r_e} = \Delta g_{fa}$$

$$\Delta g_{fa} = 0.09476 \text{ milligal/foot } h \text{ (feet),}$$

$$\Delta g_{fa} = 0.3086 \text{ milligal/meter } h \text{ (meters),}$$

where,  $g_0$  is about 980 gals.

## 2. Bouguer plate correction.

This correction implied that between the observation stations and datum, there are some materials with different densities. In this case



when the greater the distance of the observation stations are, the greater the gravity values, because the increase of the masses of the materials of density  $\rho$  between the station and datum. Bouguer plate corrections are always negative.

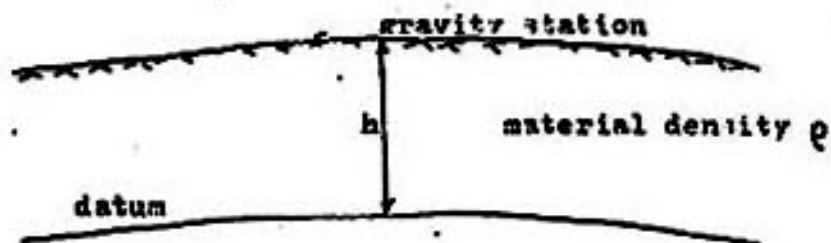


Figure 4. Diagram illustrating Bouguer plate correction .

As shown in figure 4.

Bouguer plate corrections are,

$$\Delta s_{bp} = - 2\pi\rho G h^*$$

### III. TERRAIN CORRECTIONS

Terrain correction may often be neglected in the area of small relief topography, but in the hilly country, and when the high-precision gravity surveys need, terrain correction are very importance. The effect from the terrain because of the valley below the observation stations are the attraction of the masses of materials that have to add to the valley. And the effect from terrain because of the hill above the observation stations are the attraction that have to remove the hill. Terrain corrections are

\* See appendix II.

(Heiland, 1946, p. 70). But the sample of materials may vary the value of the densities from the surface to the depth in the subsurface because the samples may come from the weathering surface or the samples at the depth in the subsurface (Hettleton, 1939).

Hettleton (1939) uses the method to determine the average density in the area of gravity survey from the surface down to the subsurface by using the gravity meter. One special traverse that is free from any minerals or the geologic features, is chosen. Because the minerals or geologic structures may produce the gravity anomalies. This traverse must cover either the hill or the valley of gently topography in order to avoid the terrain effects. The observed gravity anomalies along this traverse are corrected to the datum by the use of different values of density. The density which gives the straight line if the traverse is short, or the smooth curve if the traverse is long, is considered the best correct density value in that area of the gravity survey. This method is good for the high precision survey.

The value of the density are very importance in the gravity survey, the density of igneous rocks inverse with the composition of  $SiO_2$ . The density of the ore minerals may proportional with the composition of the ore (Heiland, 1946, p. 73).

## 2. TIDAL CORRECTIONS

The attraction of the sun and the moon are the cause of the tidal effect which may change the gravity values in the maximum amplitude of

about 0.3 milligal during the day. This effect is very small when compare with the other effects. Copel (1954) has shown the tidal effect corrections method by using the formulas and the tables which publish in advance for each year in "Geophysical prospecting magazine" in December. The tidal corrections are used when the survey needs very high accuracy. Usually, this correction can use by the drift corrections.\*

#### F. GRAVITY ANOMALIES

After all of the corrections are calculated, Bouguer gravity anomalies can be obtained by,

Bouguer gravity anomalies = observed gravity anomalies + free-air correction  
- Bouguer plate corrections + terrain corrections - theoretical gravity values.

---

\* See page 15.

## SURVEY PROCEDURE

The standard model of Worden gravity meter serial number 110 is used in this gravity survey. The instrument constant of this gravity meter is 0.0884 milligal/scale division. The accuracy of the gravity meter is about 0.01 milligal. This instrument can read in the range of about 88 milligals or 1000 scale divisions. Before each reading, the traverse and the longitudinal levels of the gravity meter must be checked very carefully. This gravity meter measured only vertical component of gravity value.

The master base station is located at RDD building of New Mexico Institute of Mining and Technology, which opposite room no. 24. The absolute gravity value of this master base station is 979185.36 milligals. This absolute gravity value is correlated to the observed gravity anomalies in the field survey. When the base station needs to transfer to the new base station, the gravity meter readings are repeated at least twice at the base station and at the new base station. All of the corrections are corrected for those readings in the same way with the other observed gravity anomalies. Station 315 and 3275 are the base stations in this gravity survey. The absolute gravity values of station 315 and 3275 are 979199.11 and 979211.85 milligals respectively.

The temperature effect, and the attraction of the sun and the moon

can be corrected by the drift corrections. The drift corrections are corrected by repeating the readings at the same base station within every two hours. The different value of two reading at the same base station is plotted against the times by setting one reading at zero, and draw the straight line between these two points. The drift correction can be determined at each station by that straight line. After the drift values are corrected to the reading gravity values from the gravity meter, observed gravity values can be obtained.\*

---

\* see appendix III

## CALCULATION OF BOUGUER ANOMALIES

### A. DATUM

*Not the real reason*  
This gravity survey uses mean sea level as a datum, in order to calculate free-air and Bouguer plate corrections conveniently. Because all of the elevation values from the description of Bench Mark and quadrangle maps of 7.5 minute series, are correlated with mean sea level.

### B. ELEVATION CORRECTIONS

Free-air correction = 0.09406 milligal/feet h (feet).

Bouguer plate correction.

$$= -2\pi\rho h.$$

In this survey, the density used for the elevation correction is the density of Precambrian basement rock. The density of Precambrian basement rock is 2.667 g/cm<sup>3</sup> (Janford, 1968, p. 1).

Therefore, where,  $\rho = 2.667 \text{ g/cm}^3$ ,

$$\Delta g_{bp} = -0.03408 \text{ milligal/feet } h \text{ (feet)}.$$

The combined free-air and Bouguer plate corrections are,

$$\begin{aligned} \Delta g_{fa} + \Delta g_{bp} &= (0.09406 - 0.03408) \text{ milligal/feet } h \text{ (feet)} \\ &= 0.05998 \text{ milligal/feet } h \text{ (feet)}. \end{aligned}$$

So, free-air and Bouguer plate corrections in this gravity survey are 0.05998 times the elevation value at each gravity station.

### C. TERRAIN CORRECTIONS

The area of this gravity survey is very small relief topography. The maximum elevation at the gravity station is 5732.25 feet from mean sea

*Known corrections  
east of  
the survey area.*

level, and the minus elevation is 4725.2 feet. So, terrain corrections in this gravity survey are neglected.

#### D. THEORETICAL GRAVITY

In this gravity survey, the gradient of theoretical gravity is used.\* The calculation of theoretical gravity by this way may be convenient because the interpreters do not have to calculate the value of  $g_{th}$  at every latitude of the gravity station.

The reference latitudes are used in this method. The reference latitude can be chosen in the gravity survey area, it depends on the quality of the survey. The interval of the reference latitudes may be 5 to 10 minutes, but in the case of more detailed survey needs, the interval of reference latitude should less than 5 minutes.

Measured the distance from the gravity stations perpendicular to the nearest reference latitude in feet, the minus signs are used for the distance when the gravity stations are located on the south of the reference latitudes. The minus sign is used because the gravity value of the earth at the pole is greater than the gravity value of the earth at the equator about 5.2 gal

The value of  $g_{th}$  can calculate from the equation,

$$g_{th} = g_{th}(\text{reference latitude}) + \frac{d}{d_s} g_{th}(\text{reference latitude}) \times \text{the distance north or south of that reference latitude in feet.}^{***}$$

\* see page 8.

\*\* see page 7.

\*\*\* see appendix I.

where,

$$g_{th}(\text{reference latitude } \phi) = 978.049(1 + .005283384 \sin^2 \phi - .000005869 \sin^2 2\phi)$$

$$\frac{d g_{th}(\text{reference latitude } \phi)}{d s} = 24.6 \times 10^{-5} \text{ milligal/foot } \sin 2\phi$$

This survey uses this method to find the values of  $g_{th}$ . The reference latitudes in this survey are  $34^{\circ} 30' N$ ,  $34^{\circ} 25' N$ , and  $34^{\circ} 20' N$ .

The values of  $\frac{d g_{th}}{d s}$  of each reference latitude are,

$$1. \frac{d g_{th}(\text{reference latitude } 34^{\circ} 30' N)}{d s} = 24.6 \times 10^{-5} \times \sin 69^{\circ} \text{ milligal/foot} \\ = 21.441 \times 10^{-5} \text{ milligal/foot.}$$

$$2. \frac{d g_{th}(\text{reference latitude } 34^{\circ} 25' N)}{d s} = 24.6 \times 10^{-5} \times \sin 68^{\circ} 50' \\ = 21.392 \times 10^{-5} \text{ milligal/foot.}$$

$$3. \frac{d g_{th}(\text{reference latitude } 34^{\circ} 20' N)}{d s} = 24.6 \times 10^{-5} \times \sin 68^{\circ} 40' \\ = 21.344 \times 10^{-5} \text{ milligal/foot.}$$

The  $g_{th}$  of each reference latitude can be calculated by the international gravity formula,

$$1. g_{th}(\text{reference latitude } 34^{\circ} 30' N) = 979703.35 \text{ milligal,}$$

$$2. g_{th}(\text{reference latitude } 34^{\circ} 25' N) = 979696.34 \text{ milligal,}$$

$$3. g_{th}(\text{reference latitude } 34^{\circ} 20' N) = 979689.34 \text{ milligal,}$$

From these values,  $g_{th}$  at each observation station can be calculated.\*

---

\* See Table I.





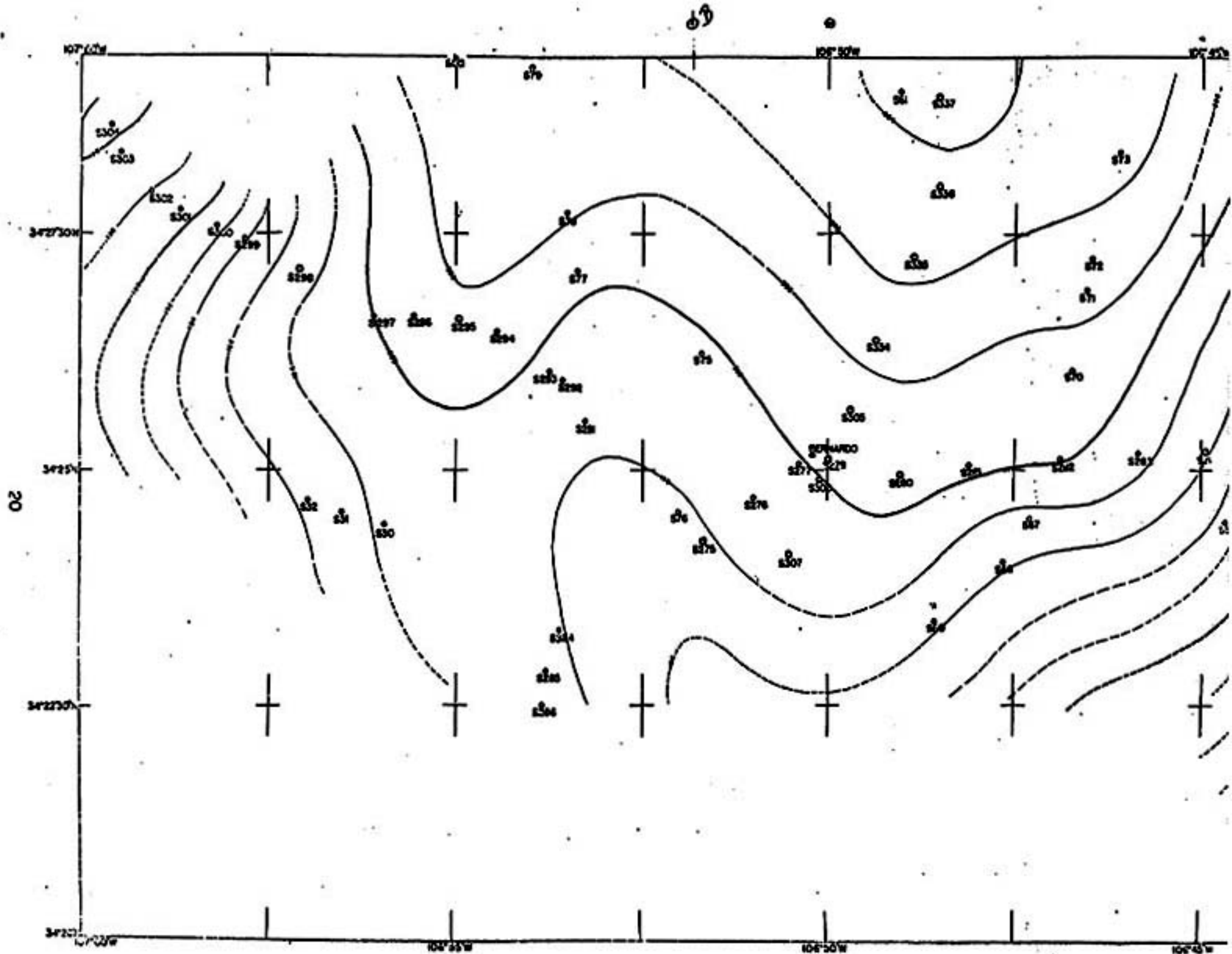


Figure 7a. Total Bouguer anomalies map.

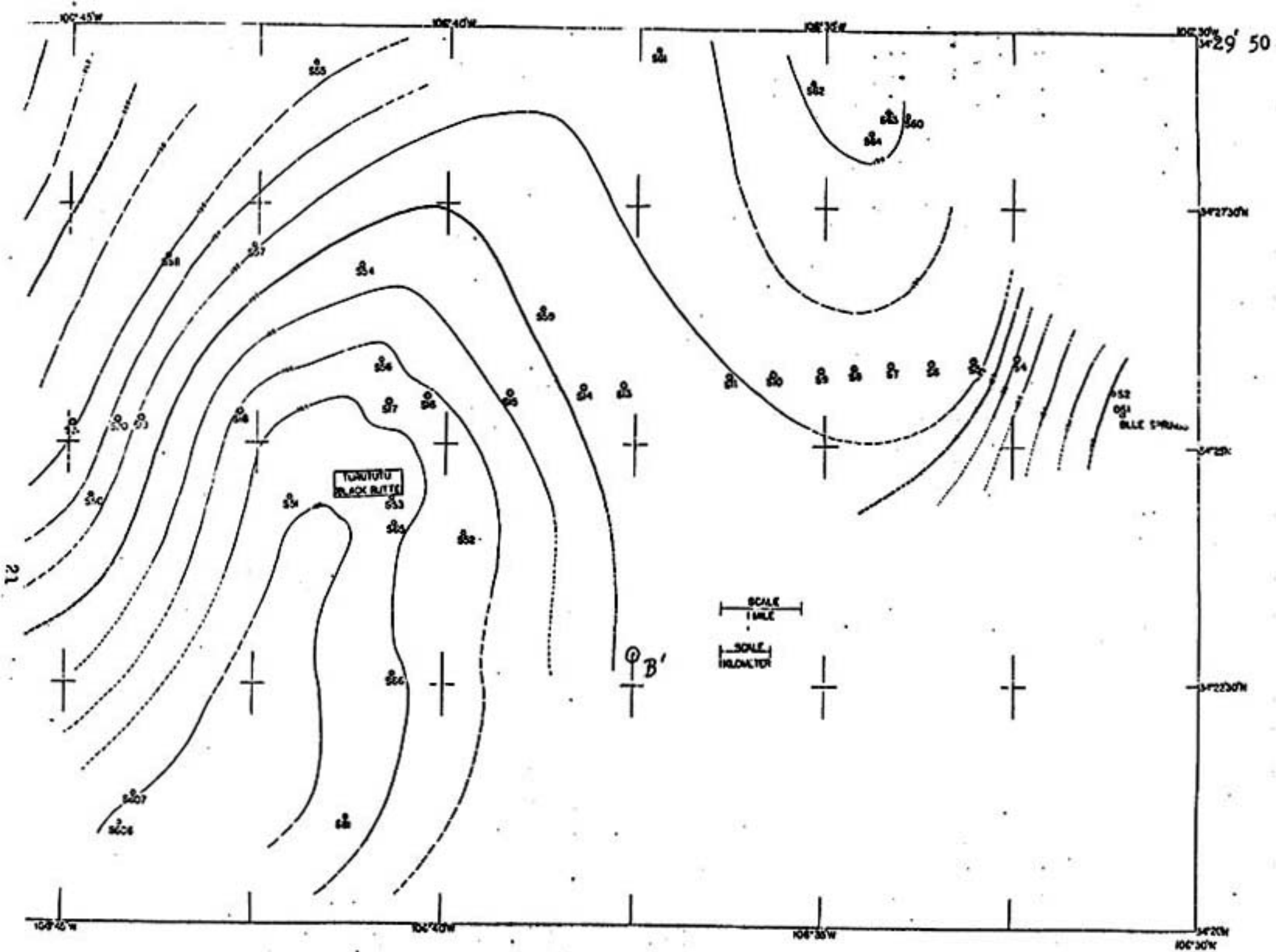


Figure 7b. Total Bouguer anomalies map.

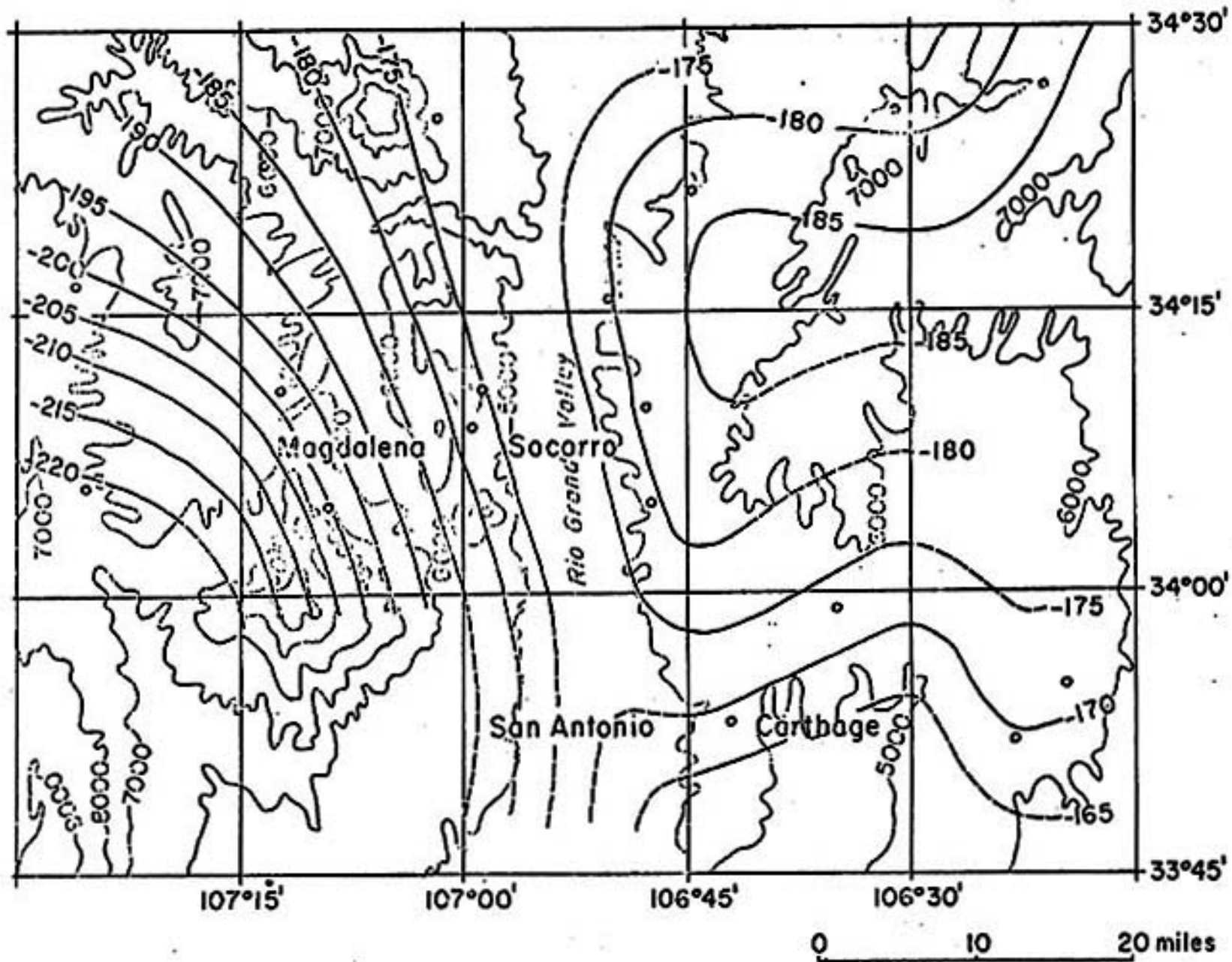


Figure 8. Regional Bouguer anomaly map.  
(From Sanford, 1968)

## BOUGUER GRAVITY MAPS

The regional Bouguer gravity anomalies map from Sanford (1968), is used in order to get the residual Bouguer anomalies map. The regional Bouguer anomalies map has been done by reading the 19 observed gravity anomalies on or near Precambrian basement rocks in the area larger than the area of gravity survey (Sanford, 1968, p. 3). Because the regional gravity is affected from the deep-seated structures. The observed gravity anomalies from that regional area are corrected by all of the corrections and geologic corrections\*, then Bouguer gravity anomalies can calculate. After that the regional Bouguer anomalies map is obtained\*\* These affects from regional gravity have to get rid of.

After the regional affects are removed off, the residual Bouguer anomalies map is obtained. The residual Bouguer anomalies map can be obtained directly subtracting the regional Bouguer anomalies map from the total Bouguer anomalies map (Sanford, 1968, p. 3).

Total Bouguer anomalies map, as shown in figure 7a, and figure 7b, have shown Bouguer anomalies contour lines of interval two milligals. Every ten milligals, the contour line is heavy line. The dashed lines will show the contour lines which are no gravity stations controlled. For the more certain contour lines, the dashed lines will be longer; for the more uncertain contour lines, the dashed lines will be shorter. The gravity stations with exact elevation values from description of Bench mark, are shown by double-circles

\* See appendix V.

\*\* See figure 8.

The gravity stations with the elevation values from quadrangle maps of 7.5 minute series, are shown by single circle.

Residual Bouguer anomalies map, as shown in figure 9, can explain in the same way with total Bouguer anomalies map. The contour line interval in this map is only one milligal, and every five milligals is shown by heavy line. The heavy dash lines of regional anomalies, (of figure 8), of contour interval five milligals are shown in this map. In this residual Bouguer anomalies map, profiles AA' and BB', which cross at Turututu, are shown. Profile AA' is a straight line between latitude  $34^{\circ} 22' N$ , longitude  $106^{\circ} 45' W$  and latitude  $34^{\circ} 29' 40'' N$ , longitude  $106^{\circ} 33' 50'' W$ . Profile BB' is a straight between latitude  $34^{\circ} 29' 40'' N$ , longitude  $106^{\circ} 51' 50'' W$  and latitude  $34^{\circ} 22' 50'' N$ , longitude  $106^{\circ} 37' 30'' W$ . This residual Bouguer anomalies map is the map using for the gravity interpretation.

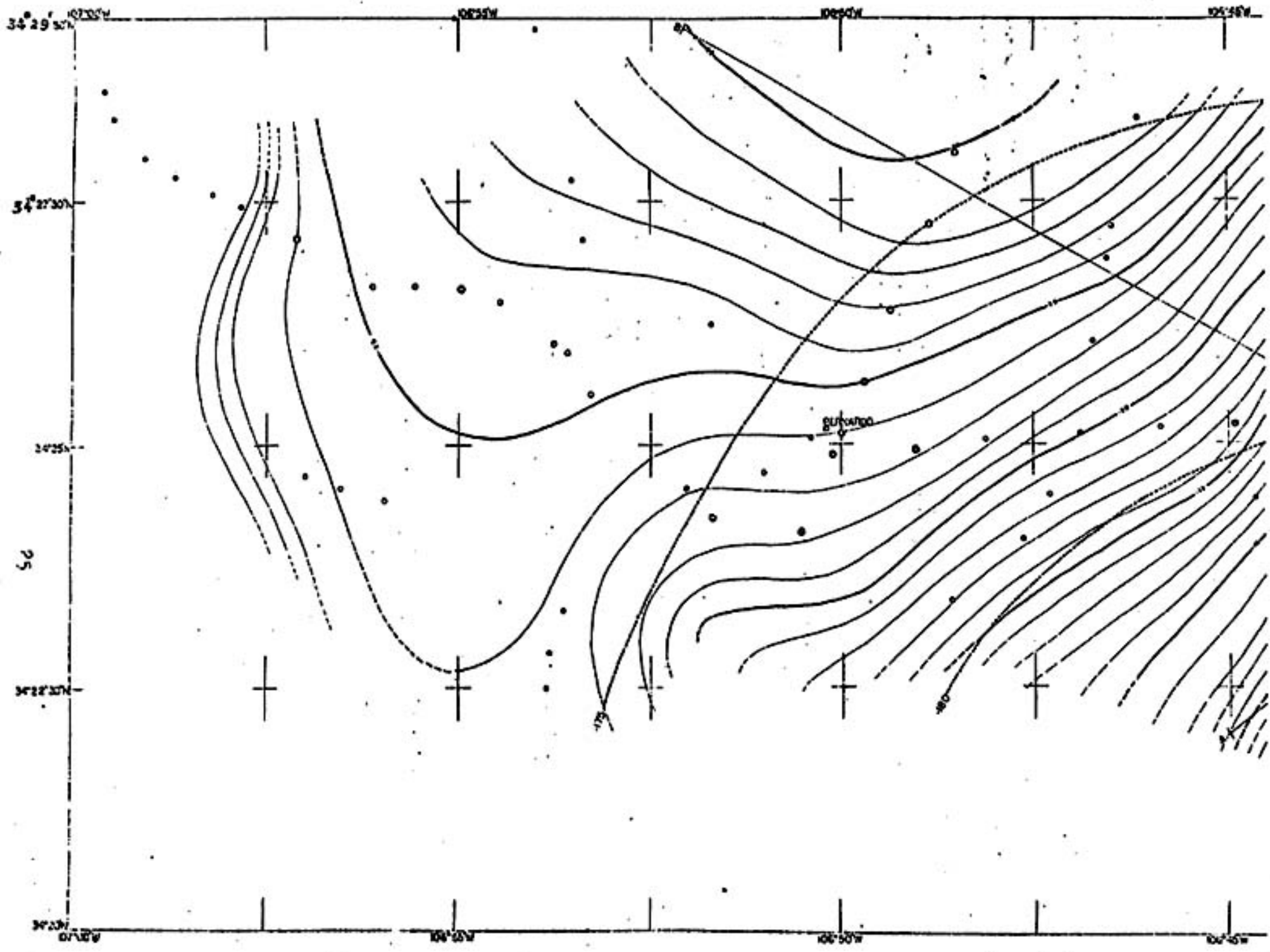


Figure 9a. Residual anomalies map.

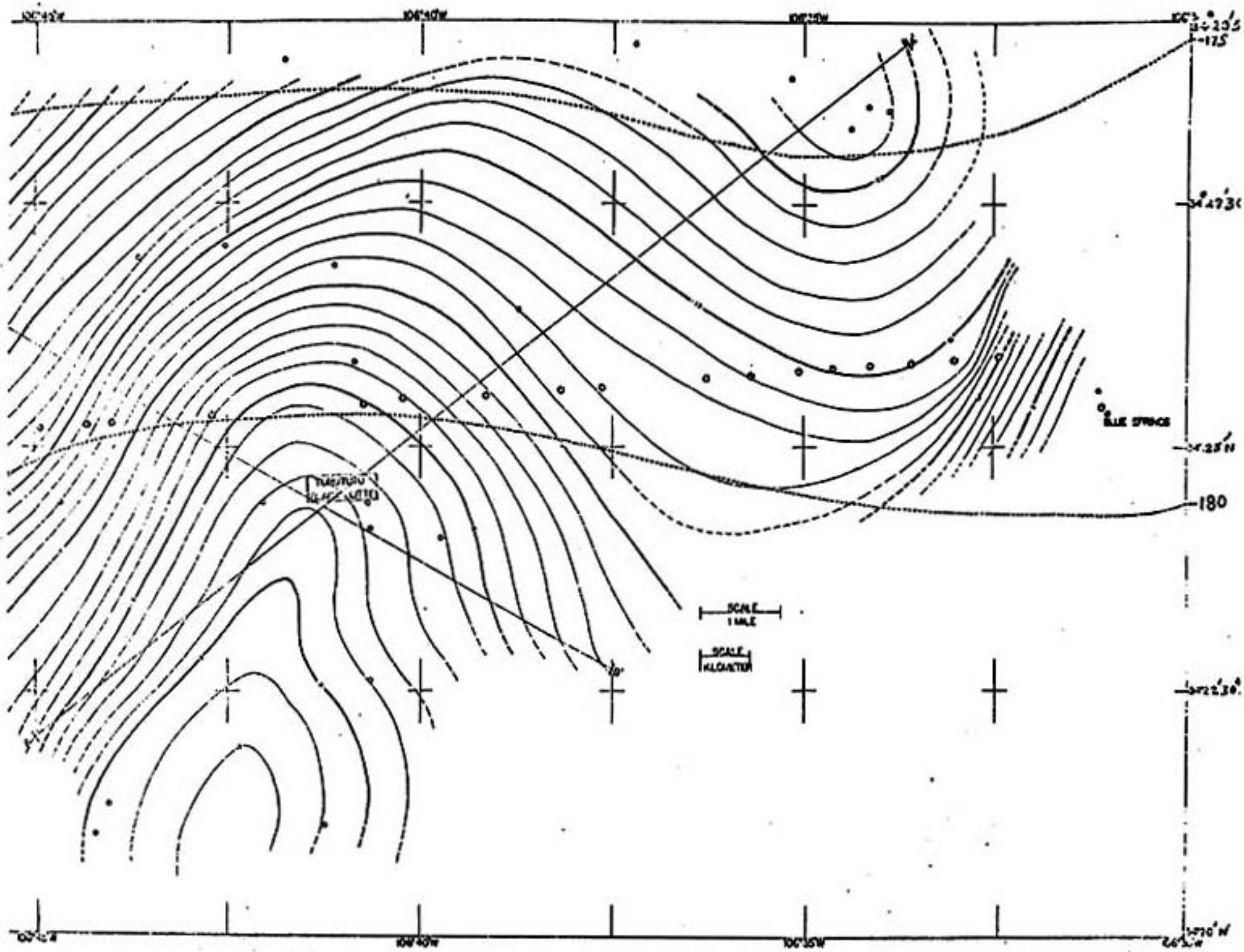


Figure 9b. Residual anomalies map.



## GEOLOGY OF THE GRAVITY SURVEY AREA

### A. STRATIGRAPHY

1. Precambrian rocks in Joyita hills, the core of Los Pinos mountains, and some parts of Jansano mountains, are composed of Sais quartzite, Blue Springs schist, White Ridge quartzite, Sevilleta rhyolite, and basic schist. The thickness of these Precambrian rocks is at least 12,000 feet (Stark and Dapples, 1946).

2. Carboniferous rocks is exposed only Pennsylvanian Series. These Series are divided into two formations.

a. Sandia formation which is the oldest rocks of Carboniferous age. this formation is exposed only an upper clastic member of the thickness about 100 feet in Joyita hills and 350 feet in the core of Los Pinos mountains.

b. Madera Limestone is composed of two member. The thickness of Lower grey limestone member is about 80 feet in Joyita hills and 830 feet in the east central of Los Pinos. The thickness of Arkovic limestone member is about 520 feet in the south of Los Pinos mountains.

3. Permian rocks are divided into two formations from the identification of the fossils.

a. Barsum formation has the thickness from 28 to 234 feet.

b. Abo formation has the thickness of about 370 feet in Joyita hill.

According to the graphic sections, Permian rocks can be divided into Gato and San Andres formations.

- a. Yaso formation, is divided into 4 member,
  - 1. Lower or Jaxeta Blanca sandstone member has the thickness of 104 to 222 feet,
  - 2. Torres member has the thickness of about 350 to 600 feet,
  - 3. Canas gypsum member has the thickness of about 103 feet,
  - 4. Joyita sandstone member has the thickness of 60 to 90 feet.
- b. San Andreas formation is divided into 3 members,
  - 1. Glorieta sandstone member has the thickness of 140 to 170 feet.
  - 2. Limestone member has the thickness of 270 to 280 feet.
  - 3. Upper member has the thickness of 5 to 18 feet.
- 4. Triassic rocks are composed of Dockum formation of the thickness about 500 feet.
- 5. Cretaceous rocks are divided into 3 formations.
  - a. Dakota sandstone formation has the thickness of about 12 feet,
  - b. Mancos formation has the thickness of about 200 feet,
  - c. Mesaverde formation has the thickness of about 200 feet.
- 6. Tertiary rocks are divided into 3 formations.
  - a. Baca formation has the thickness of 80 to 140 feet.
  - b. Datil formation has the thickness of about 2000 feet. This formation is exposed near Joyita hills which locate on the southern part of this gravity survey. It is not exposed in the gravity survey.
  - c. Santa fe formation is varied in the thickness. So, the thickness of this formation will be interpreted in this gravity survey.
- 7. Quaternary rocks is the gravel and alluvium which will be interpreted the thickness in this gravity survey.

These information of stratigraphy are come from Wilbalt, (1946).

## B. STRUCTURE

Most of the mountains of New Mexico are in the trend of north-south. The area of this gravity survey is in the southern end of Albuquerque-Belen basin. Ladron mountains are located on the west; and Manzano mountains, Los Pinos mountains, Joyita hills are located on the east, at the margin of the basin. The trend of these mountains are about N 20° E. The width of Albuquerque-Belen basin is about 30 miles. In this basin, Precambrian surface is at the depth of about 10,000 to 15,000 feet, (and more further to the north), below mean sea level (Kelly, 1953, p. 95-96).

In the Ladron mountains, Precambrian rocks are in contact with Tertiary volcanic rocks and Santa Fe sediments, because of Cerro Colorado normal fault at the eastern face. Pre-Santa Fe beds of red and gray sandstones, shale, limestone, and bed of gypsum are exposed at the west slope of Ladron mountains (Denny, 1941).

Paloma thrust fault begins from the southern end of Manzano mountains and this thrust fault occurs along the whole length of Los Pinos mountains in the direction of about N 18° E and dip to the west of the angle about 40° to 50°. Montosa thrust fault is located on the western side of Paloma thrust fault, this fault begins at the north of Abo Pass which is the distance about  $\frac{1}{2}$  mile from Paloma thrust fault. The lower grey limestone member and Arkotic limestone member of Madera limestone of Pennsylvanian series are in contact with Precambrian rocks in Los Pinos mountains, because of Paloma thrust fault. Paloma and Montosa thrust faults are nearly parallel with Los Pinos gravity fault. This gravity fault is located to the

west of Montosa and Paloma thrust faults (Stark and Dapples, 1946).

Joyita hills are tilted horsts, which are bounded by the west and the east Joyita gravity faults. Datil formation of Tertiary age covered the eastern part of Joyita hills because the effect of the down-faulting from the east Joyita fault. This east Joyita fault might extend to the north nearly parallel to the direction of Los Pinos gravity fault (Wilpolt, 1946).

Because of Paleozoic rocks in Joyita hills, the area between Joyita hills and Los Pinos mountains, dip to the north underly Santa Fe formation. The depth of Santa Fe formation will be increased in the area far away to the north, and might be shallow in the area near Turututu, Manzano mountains, and Los Pinos mountains.

## INTERPRETATION

### A. QUALITATIVE INTERPRETATION

All of Bouguer anomalies in this gravity survey are negative as shown in Table I, because the average elevation of this area is above mean sea level. Heiskanen and Vening Meinesz (1958, p. 147), explain that in the mountain area above mean sea level, Bouguer anomalies are negative; in the level land, near mean sea level, Bouguer anomalies are nearly zero; and in the ocean below mean sea level, Bouguer anomalies are positive. This is from the concept of isostasy.

From the residual Bouguer anomalies map as shown in figure 9, the gravity anomalies in the mountains are more greater than the gravity anomalies in Rio Grande depressions. Because the average density of Quaternary and Santa Fe formation of rocks is about  $2.2 \text{ gram/cm}^3$ , but the density of Precambrian basement rocks at Manzano mountains and Los Pinos mountains are about  $2.667 \text{ gram/cm}^3$ .

The gravity anomalies also depend on the mass and density of the materials underneath the gravity stations, if the mass of materials are closed to the gravity stations, or the density of that materials are large, the gravity anomalies of those gravity stations will greater than the gravity anomalies when the mass of materials are far away, or the density of that materials are small. If the gravity stations are vertically above the mass of materials, the gravity anomalies of those gravity stations will greater than the gravity anomalies when the stations are not above the mass of materials (Grant and Keet, 1965, p. 212). So, in this gravity survey, at the area closes to Turututu, as shown in figure 9, the gravity

TABLE I BOUGUER GRAVITY

station	reference latitude	dist. N or S of ref. lat. ft.	*	$\epsilon_{th}$ of ref. lat.** 979-	$\epsilon_{th}$ 979-***
S1	34° 25' N	+ 2,400	+0.513	696.34	696.853
S2	34° 25' N	+ 3,500	+0.749	696.34	697.089
S4	34° 25' N	+ 5,675	+1.214	696.34	697.554
S5	34° 25' N	+ 5,500	+1.176	696.34	697.516
S6	34° 25' N	+ 5,250	+1.123	696.34	697.463
S7	34° 25' N	+ 5,100	+1.091	696.34	697.431
S8	34° 25' N	+ 4,925	+1.053	696.34	697.393
S9	34° 25' N	+ 4,800	+1.027	696.34	697.367
S10	34° 25' N	+ 4,500	+0.963	696.34	697.303
S11	34° 25' N	+ 4,325	+0.925	696.34	697.265
S13	34° 25' N	+ 3,850	+0.823	696.34	697.163
S14	34° 25' N	+ 3,675	+0.786	696.34	697.126
S15	34° 25' N	+ 3,275	+0.700	696.34	697.040
S16	34° 25' N	+ 3,025	+0.647	696.34	696.987
S17	34° 25' N	+ 2,725	+0.583	696.34	696.923
S18	34° 25' N	+ 2,050	+0.438	696.34	696.778
S19	34° 25' N	+ 1,650	+0.353	696.34	696.693
S20	34° 25' N	+ 1,350	+0.289	696.34	696.629
S21	34° 25' N	+ 1,225	+0.262	696.34	696.602
S30	34° 25' N	- 3,250	-0.695	696.34	695.645
S31	34° 25' N	- 2,450	-0.524	696.34	695.816
S32	34° 25' N	- 1,750	-0.374	696.34	695.966

## EXPLANATION OF TABLE I

\* Distance of north or south of reference latitude  $\times \frac{d}{s} \epsilon_{th}$  (reference latitude), see page 17.

\*\* See page 18.

\*\*\*  $\epsilon_{th} = \epsilon_{th}(\text{reference latitude}) + \frac{d}{s} \epsilon_{th}(\text{reference latitude})$

$\times$  Dist. of N or S of reference latitude, see page 17.

\*\*\*\* elevation above mean sea level  $\times 0.05998$

\*\*\*\*\*  $\epsilon_{\text{Bouguer}} = \text{observed gravity value} + \text{free-air and Bouguer}$

plate corrections - theoretical.

## ALIFS AND CORRECTION

reduced gravity J79-	elevation above MSL, feet	**** free-air and bouguer plate correction	**** E bouguer
174.013	5,732.25	343.820	-179.002
175.360	5,705	342.186	-179.543
182.116	5,472.09	328.216	-187.222
179.803	5,435.23	326.005	-191.708
131.318	5,389.006	323.236	-192.909
184.653	5,335.84	320.044	-192.734
186.477	5,309.36	318.455	-192.461
187.398	5,281.48	316.783	-193.186
189.603	5,246.414	314.680	-193.020
192.365	5,219.47	313.064	-191.836
195.246	5,183.80	310.924	-190.993
195.439	5,177.00	310.516	-191.171
199.112	5,152.046	309.020	-188.908
203.995	5,122.34	307.238	-185.754
203.957	5,126.887	307.511	-185.455
207.752	5,061	303.559	-185.467
206.781	4,970.68	298.141	-191.771
204.284	4,982.93	298.876	-193.469
200.913	4,989.792	299.238	-196.401
192.877	5,079	304.638	-198.430
190.586	5,141	308.357	-196.873
187.951	5,199	311.836	-196.215

TABLE I (continued).

station	reference latitude	dist. N or S of ref. lat. ft.	*	h <sup>th</sup> of ref. lat.** 979-	ε <sub>th</sub> 979-***
S50	34° 25' N	- 3,350	-0.717	696.34	695.623
S51	34° 25' N	- 3,400	-0.727	696.34	695.613
S52	34° 25' N	- 5,600	-1.198	696.34	695.142
S53	34° 25' N	- 3,450	-0.738	696.34	695.602
S54	34° 25' N	+11,200	+2.396	696.34	698.736
S55	34° 30' N	- 6,250	-1.340	703.35	702.010
S56	34° 25' N	+ 5,350	+1.144	696.34	697.484
S57	34° 25' N	+12,450	+2.663	696.34	699.003
S58	34° 25' N	+11,950	+2.556	696.34	698.896
S59	34° 25' N	+ 8,500	+1.829	696.34	698.169
S60	34° 30' N	- 9,250	-1.983	703.35	701.376
S61	34° 30' N	- 5,150	-1.104	703.35	702.264
S62	34° 30' N	- 7,250	-1.554	703.35	701.796
S63	34° 30' N	- 8,975	-1.924	703.35	701.426
S64	34° 30' N	-10,350	-2.219	703.35	701.131
S65	34° 25' N	- 5,000	-1.070	696.34	695.270
S66	34° 25' N	-14,500	-3.102	696.34	693.238
S67	34° 25' N	- 3,150	-0.674	696.34	695.666
S68	34° 25' N	- 5,800	-1.241	696.34	695.099
S69	34° 25' N	- 9,800	-2.096	696.34	694.244
S275	34° 25' N	- 4,500	-0.963	696.34	695.377
S70	34° 25' N	+ 6,500	+1.390	696.34	697.730
S71	34° 25' N	+11,600	+2.481	696.34	698.821
S72	34° 25' N	+13,550	+2.899	696.34	699.239
S73	34° 30' N	- 9,975	-2.139	703.35	701.211
S74	34° 30' N	- 4,050	-0.868	703.35	702.482
S75	34° 25' N	+ 7,600	+1.626	696.34	697.966
S76	34° 25' N	- 2,550	-0.545	696.34	695.795
S77	34° 25' N	+12,750	+2.727	696.34	699.067
S78	34° 30' N	-13,700	-2.937	703.35	700.413
S79	34° 30' N	- 4,500	-0.975	703.35	702.375
S80	34° 30' N	- 3,800	-0.815	703.35	702.535
S81	34° 30' N	- 6,100	-1.308	703.35	702.042
S82	34° 20' N	+ 6,800	+1.451	689.34	690.791

See explanation in page 32.



observed gravity 979-	elevation above MSL, feet	**** free-air and bouguer plate corrections	***** E bouguer
203.205	4,990	299.300	-193.118
209.986	5,058	303.379	-182.248
201.793	5,139	308.237	-185.112
204.560	5,134	307.937	-183.105
205.939	5,067	303.919	-188.878
203.547	5,028	301.579	-196.884
205.722	5,104	306.138	-185.624
206.189	5,009	300.440	-192.374
205.645	4,955	297.201	-196.050
196.702	5,172	310.216	-191.251
187.545	5,299	317.834	-195.988
198.864	5,184	310.936	-192.446
190.329	5,253	315.075	-196.392
188.045	5,288	317.174	-196.207
187.593	5,288	317.174	-196.364
205.821	5,112	306.618	-183.831
183.204	5,190	311.296	-183.738
210.995	4,789	287.244	-197.427
212.081	4,782	286.824	-196.194
213.519	4,742	284.425	-196.300
211.850	4,760.542	285.537	-197.990
209.864	4,773	286.284	-201.582
210.549	4,759	285.445	-202.827
210.739	4,753	285.085	-203.415
209.359	4,781	286.764	-205.088
211.412	4,769	286.045	-205.025
213.028	4,772	286.224	-198.714
211.642	4,776	286.464	-197.653
211.571	4,786	287.064	-200.432
211.154	4,784	286.944	-202.315
208.947	4,844	290.543	-202.885
206.378	4,889	293.242	-202.915
208.864	4,828	289.583	-203.595
191.313	5,269	316.035	-183.443

TABLE I (continued).

station	reference latitude	dist. N or S of ref. lat. miles	*	$\epsilon_{th}$ of ref. lat.**	$\epsilon_{th}$ 979***
S276	34° 25' N	-0.34	-0.41	696.34	695.30
S277	34° 25' N	-0.10	-0.12	696.34	696.22
S279	34° 25' N	+0.15	+0.18	696.34	696.52
S280	34° 25' N	-0.03	-0.04	696.34	696.30
S281	34° 25' N	+0.08	+0.10	696.34	696.44
S282	34° 25' N	+0.14	+0.17	696.34	696.51
S283	34° 25' N	+0.21	+0.26	696.34	696.60
S284	34° 25' N	-1.97	-2.40	696.34	693.94
S285	34° 25' N	-2.43	-2.96	696.34	693.38
S286	34° 25' N	-2.86	-3.49	696.34	692.85
S291	34° 25' N	+0.63	+0.77	696.34	697.11
S292	34° 25' N	+1.11	+1.35	696.34	697.69
S293	34° 25' N	+1.22	+1.49	696.34	697.73
S294	34° 25' N	+1.72	+2.10	696.34	698.44
S295	34° 25' N	+1.83	+2.23	696.34	698.57
S296	34° 25' N	+1.87	+2.28	696.34	698.62
S297	34° 25' N	+1.89	+2.30	696.34	698.64
S298	34° 25' N	+2.49	+3.03	696.34	699.37
S299	34° 25' N	+2.86	+3.49	696.34	699.83
S300	34° 30' N	-2.73	-3.33	703.35	700.02
S301	34° 30' N	-2.52	-3.07	703.35	700.28
S302	34° 30' N	-2.31	-2.82	703.35	700.53
S303	34° 30' N	-1.83	-2.23	703.35	701.12
S304	34° 30' N	-1.51	-1.84	703.35	701.51
S305	34° 25' N	+0.77	+0.94	696.34	697.23
S306	34° 25' N	-0.10	-0.12	696.34	696.22
S307	34° 25' N	-1.02	-1.24	696.34	695.10
S334	34° 25' N	+1.61	+1.96	696.34	698.30
S335	34° 25' N	+2.62	+3.19	696.34	699.53
S336	34° 30' N	-2.28	-2.78	703.35	700.57
S337	34° 30' N	-1.21	-1.48	703.35	701.87
S606	34° 20' N			689.34	
S607	34° 20' N			689.34	

See explanation in page 32.

observed gravity 979-	elevation above MSL, feet	free-air and bouguer plate corrections	**** **** K <sub>bouguer</sub>
212.36	4,748	284.79	-198.78
212.16	4,742	284.43	-199.63
211.64	4,738.5	284.22	-200.66
211.68	4,725.2	283.42	-201.20
212.14	4,732	283.83	-200.47
207.30	4,821	289.16	-200.05
203.89	4,904	294.14	-198.57
199.48	4,941	296.36	-198.10
197.23	4,963	297.67	-198.48
193.97	5,002	300.02	-198.86
209.72	4,822	289.22	-198.17
208.71	4,826	289.46	-199.52
208.20	4,840	290.30	-199.23
201.36	4,927	295.52	-201.56
199.03	4,965.1	297.81	-201.73
196.92	5,009	300.44	-201.26
195.96	5,045	302.60	-200.08
195.41	5,112.9	306.67	-197.29
196.80	5,155	309.20	-193.83
197.22	5,195	311.60	-191.20
197.49	5,231	313.76	-189.13
196.92	5,262	315.61	-188.00
195.27	5,285	316.99	-188.86
194.44	5,272	316.21	-190.86
211.73	4,740	284.31	-201.24
212.64	4,729.4	283.67	-199.91
212.00	4,736.8	284.11	-198.99
211.69	4,738.8	284.23	-202.38
210.99	4,734.64	283.98	-204.61
211.92	4,742.77	284.47	-204.18
211.70	4,773.13	286.29	-203.87
195.53	5,236	314.06	-181.18
194.09	5,238	314.18	-182.93

anomalies are greater than the gravity anomalies of Rio Grande depressions, and of the mountains of Precambrian basement rocks. Because of the intrusive basalt rocks of density about  $3.00 \text{ gram/cm}^3$  at Turututu.

The narrow space of Bouguer anomaly contours obviously show the fault which lies on the west of Manzano and Los Pinos mountains, at about latitude  $34^{\circ} 25' \text{ N}$ , longitude  $106^{\circ} 32' 30'' \text{ W}$ , in the direction of  $\text{N } 30^{\circ} \text{ E}$  and  $\text{S } 30^{\circ} \text{ W}$ . This fault is in contact with Santa Fe formation of Tertiary age and Precambrian basement rocks. No evidence of any faults in the area closer to Turututu, the intrusive basalt of Turututu might be exposed by the volcanic activity.

The relatively wide Bouguer anomaly contour of maximum negative at about latitude  $34^{\circ} 29' 50'' \text{ N}$ , longitude  $106^{\circ} 50' \text{ W}$  to latitude  $34^{\circ} 22' 30'' \text{ N}$ , longitude  $106^{\circ} 55' \text{ W}$ , shows Rio Grande depressions. This depressions spread out to the west at about latitude  $34^{\circ} 27' 30'' \text{ N}$ , longitude  $106^{\circ} 57' 30'' \text{ W}$ , in the area of narrow space Bouguer anomaly contour which probably shows the fault (Sanford, 1968, p. 3).

The north-eastern part of the residual anomalies map also shows the depressions which is more shallower than Rio Grande depressions. This depression will extend to the south-east and is in contact with the fault.

## B. QUANTITATIVE INTERPRETATION

The geologic section from Sanford (1968), as shown in figure 10, is used for the interpretation in this gravity survey. This geologic section is divided into 7 sections, from base of Sandia formation (Pennsylvanian) to the top of Datil formation (Oligocene). Each section has the thickness of 1000 feet with average density.

This interpretation has been done under the following assumptions,

1. the geologic section of the gravity survey area is given,
2. the geologic structures are two dimensional,
3. the rock units are horizontal.

The depth to the center of displacement of vertical fault can be calculated from Bouguer anomalies profile which cross perpendicular to the strike of the vertical fault, as shown in appendix IV.

The thickness of Quaternary and Santa Fe formation can be calculated, if assumed that the intrusive basalt at Turututu is bounded by the vertical fault. Along the profile AA', the minimum negative Bouguer anomalies is -0.6 milligal. In that area, Bouguer anomalies on the Precambrian basement rocks is about 0 milligal. This value shows that the gravity effect from the rocks which overly on Precambrian basement rocks at Turututu is only 0.6 milligal. The density of basalt rocks are about  $3.0 \text{ gram/cm}^3$ , this density value is very high when compare with the density of country rocks. So, it means that the thickness of rocks which overly Precambrian basement rocks are very thin. The calculation from geologic corrections will show that Bouguer anomalies of about 1 milligal will come from the affect

\* See appendix V.

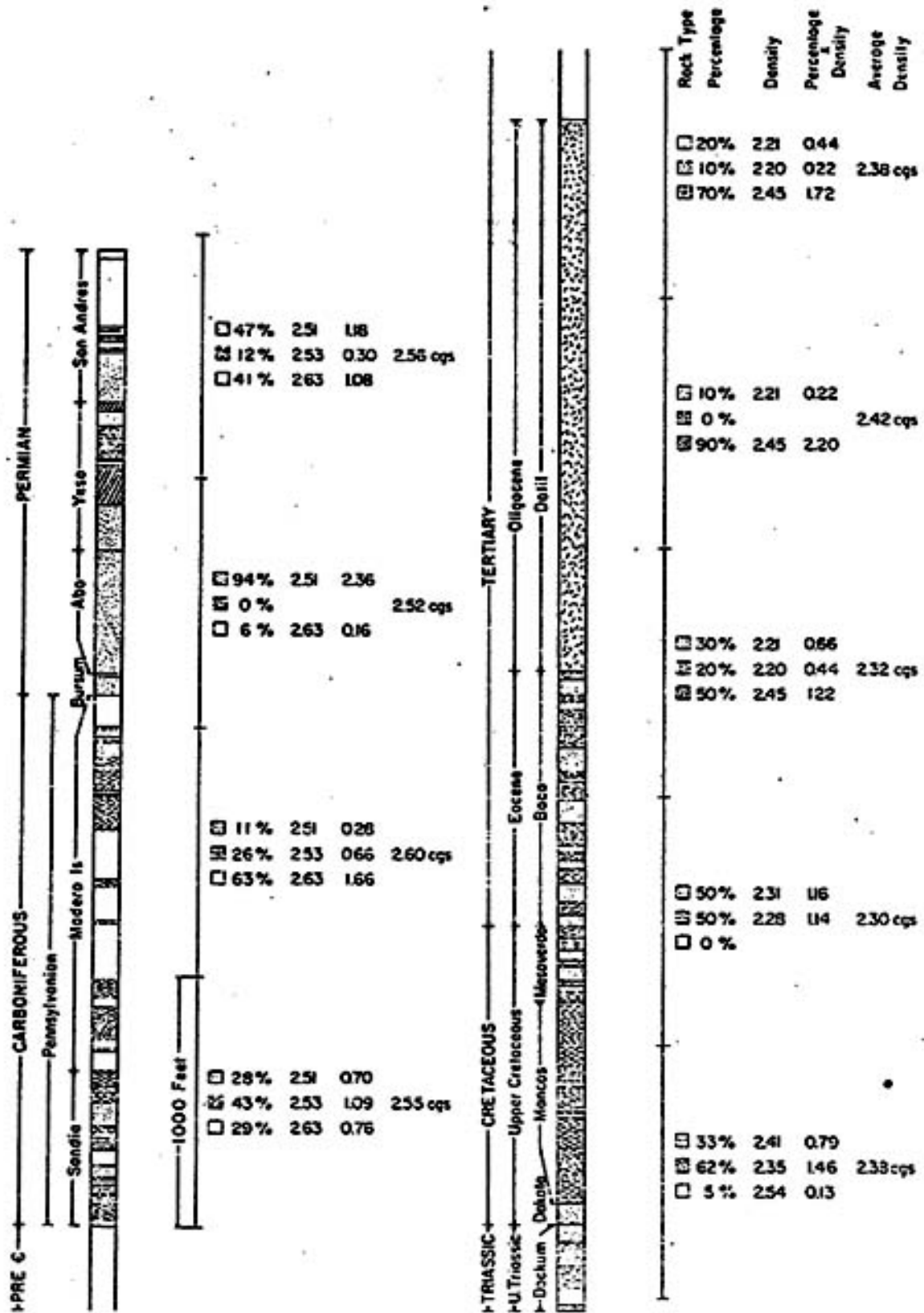


Figure 10. Geologic section used in gravity interpretation.  
(From Sanford, 1968)

of the rock of thickness about 500 feet. The thickness of Quaternary and Santa Fe formation can calculate only on the hanging wall of the fault, if assumed that Turututu is the horst structure. From the geologic section, the gravity value of each section, from the base of Sandia formation to the top of Baca formation, (Datil formation is not exposed in this area), can calculate by using Bouguer plate correction formular, and the density contrast between the density of each section and the density of Precambrian basement rocks.

$$g = 2\pi\rho G h \text{ milligal,}$$

$$g = 0.01276 \rho h \text{ milligal.}$$

Section 1. (Sandia),  $h = 1000$  feet,  $\rho = 2.667 - 2.55 = 0.117 \text{ gram/cm}^3$ .

$$g = 1.49 \text{ milligal.}$$

Section 2. (Madera),  $h = 1000$  feet,  $\rho = 2.667 - 2.60 = 0.067 \text{ gram/cm}^3$ .

$$g = 0.85 \text{ milligal.}$$

Section 3. (Gursum, Abo, Yezo),  $h = 1000$  feet,  $\rho = 2.667 - 2.52 = 0.147 \text{ gram/cm}^3$ .

$$g = 1.87 \text{ milligal.}$$

Section 4. (Yezo, Jan Andres),  $h = 1000$  feet,  $\rho = 2.667 - 2.56 = 0.107 \text{ gram/cm}^3$ .

$$g = 1.36 \text{ milligal.}$$

Section 5. (Dockum, Dakota, Mancos),  $h = 1000$  feet.

$$\rho = 2.667 - 2.38 = 0.287 \text{ gram/cm}^3.$$

$$g = 3.66 \text{ milligals.}$$

Section 6 (Desaverde, Baca),  $h = 1000$  feet,  $\rho = 2.667 - 2.30 = 0.367 \text{ gram/cm}^3$ .

$$g = 4.68 \text{ milligals.}$$

Section 7. (Baca),  $h = 1000$  feet,  $\rho = 2.667 - 2.32 = 0.347 \text{ gram/cm}^3$ .

$$g = 2.21 \text{ milligals.}$$

The total gravity values effect from the base of Sandia formation to the top of Taca formation is,

$$= 1.49 + 0.85 + 1.87 + 1.36 + 3.66 + 4.68 + 2.21 = 16.12 \text{ milligals.}$$

The different of the maximum and minimum negative Bouguer anomalies of profile AA' is  $21.5 - 0.6 = 20.9$  milligals.

Therefore the gravity value affects by Quaternary and Santa Fe formation is,

$$20.9 - 16.12 = 4.78 \text{ milligals.}$$

Therefore,  $4.78 = 0.01276 \times \text{thickness of Quaternary and Santa Fe formation}$   
 $\times (2.667 - 2.2),$

The thickness of Quaternary and Santa Fe formation near Mancano mountains is

$$\frac{4.78}{0.01276 \times 0.467} = 797 \text{ feet,}$$

where, the density of Quaternary and Santa Fe formation is  $2.2 \text{ g/cm}^3$ .

The different of the maximum and minimum negative Bouguer anomalies of profile BB' is  $30.4 - 1.5 = 28.9$  milligals.

Therefore the gravity value affects by Quaternary and Santa Fe formation is,

$$28.9 - 16.12 = 12.78 \text{ milligals.}$$

Therefore,  $12.78 = 0.01276 \times \text{thickness of Quaternary and Santa Fe formation}$   
 $\times (2.667 - 2.2).$

The thickness of Quaternary and Santa Fe formation of Rio Grande valley is,

$$\frac{12.78}{0.01276 \times 0.467} = 2130 \text{ feet.}$$



The gravity anomalies can compute by using the two dimensional gravity model program (Heckart, 1968). The layer of model in this program must be n-sided polygonal shape. Each model can construct with many layers. The density contrast between the density of the layer and the density of the surrounding formation has been used. The coordinate of every point of n-sided polygon must be known (Talwani and et al., 1959).

Vertical component of gravitation attraction due to a two dimensional body is,

$$2 G \rho \int z d \theta.$$

As shown in figure 11,

$$z = x \tan \theta,$$

$$z = (x - a_i) \tan \phi_i,$$

therefore,

$$z = \frac{a_i \tan \theta \tan \phi_i}{\tan \phi_i - \tan \theta}$$

or,

$$Z_i = \int_{\theta} z d \theta = \int_{\theta} \frac{a_i \tan \theta \tan \phi_i}{\tan \phi_i - \tan \theta} d \theta.$$

Therefore,  $V = 2 G \rho \sum_{i=1}^n Z_i,$

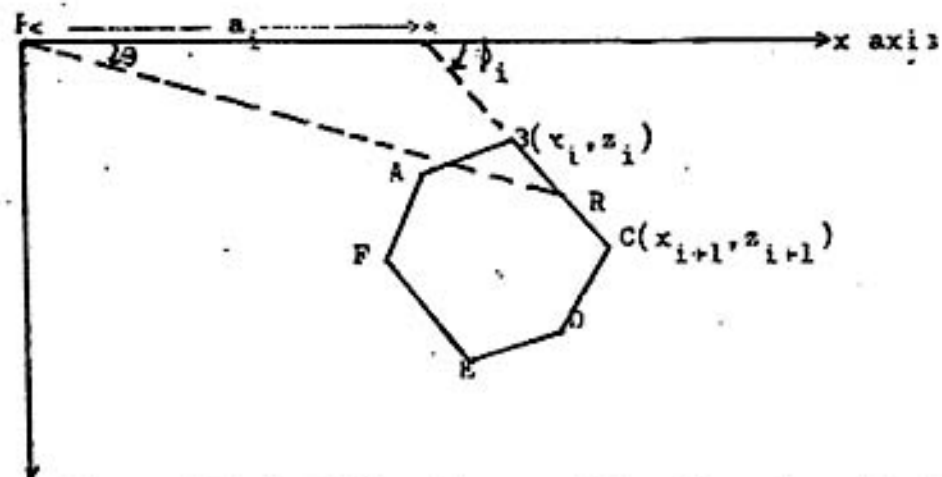


Figure 11. N-sided polygon of two dimensional body.  
(from Talwani and et al., 1959)

$$Z_i = a_i \sin \phi_i \cos \phi_i \left[ \theta_i - \theta_{i+1} + \tan \phi_i \ln \frac{\cos \theta_i (\tan \theta_i - \tan \phi_i)}{\cos \theta_{i+1} (\tan \theta_{i+1} - \tan \phi_i)} \right]$$

where,  $\theta_i = \tan^{-1} \frac{z_i}{x_i}$ ,

$$\phi_i = \tan^{-1} \frac{z_{i+1} - z_i}{x_{i+1} - x_i}$$

$$\theta_{i+1} = \tan^{-1} \frac{z_{i+1}}{x_{i+1}}$$

$$z_i = x_{i+1} + z_{i+1} \frac{x_{i+1} - x_i}{x_i - z_{i+1}}$$

The constructed models with observed gravity anomalies and computed gravity anomalies, of profile AA' and BB', are plotted by computer, as shown in figure 12 and 13 respectively. The computed gravity anomalies of profile AA' and BB' are shown in Table II.

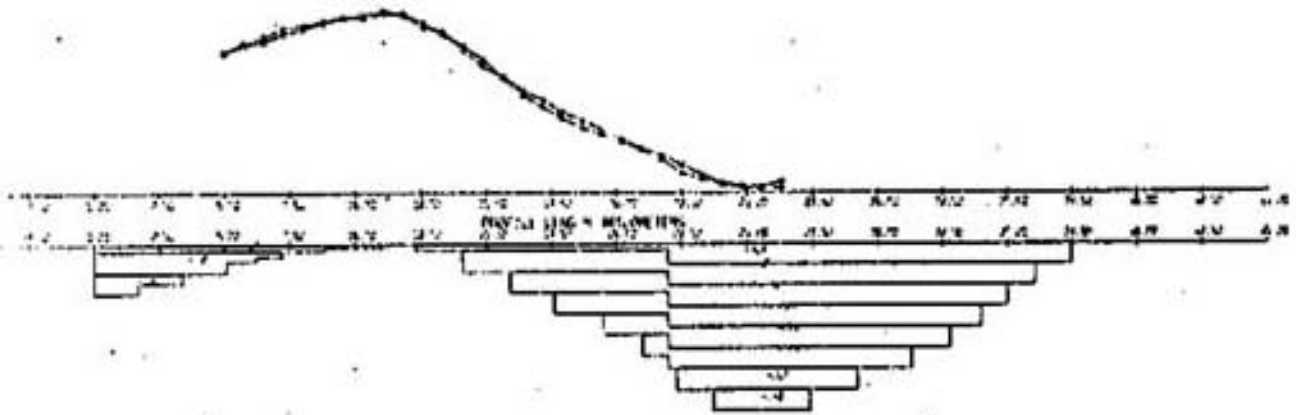
The hypothetical geologic section along profile AA' and profile BB', with observed and computed gravity anomalies are shown in figure 14 and figure 15 respectively. From these figures, show the maximum thickness of quaternary and Santa Fe formation in Rio Grande valley about 2500 feet, and the maximum thickness of depression at Abo Arroyo about 950 feet. These values of thickness when compare with the thickness from the calculation are very close.\* Two dimensional gravity models do not show any evidence of fault in the area at Turitutu. The model of profile BB' shows that the depth to Precambrian basement rocks is about 9000 feet in Rio Grande valley, and the depth of Precambrian basement rocks will be

\* See page 39.

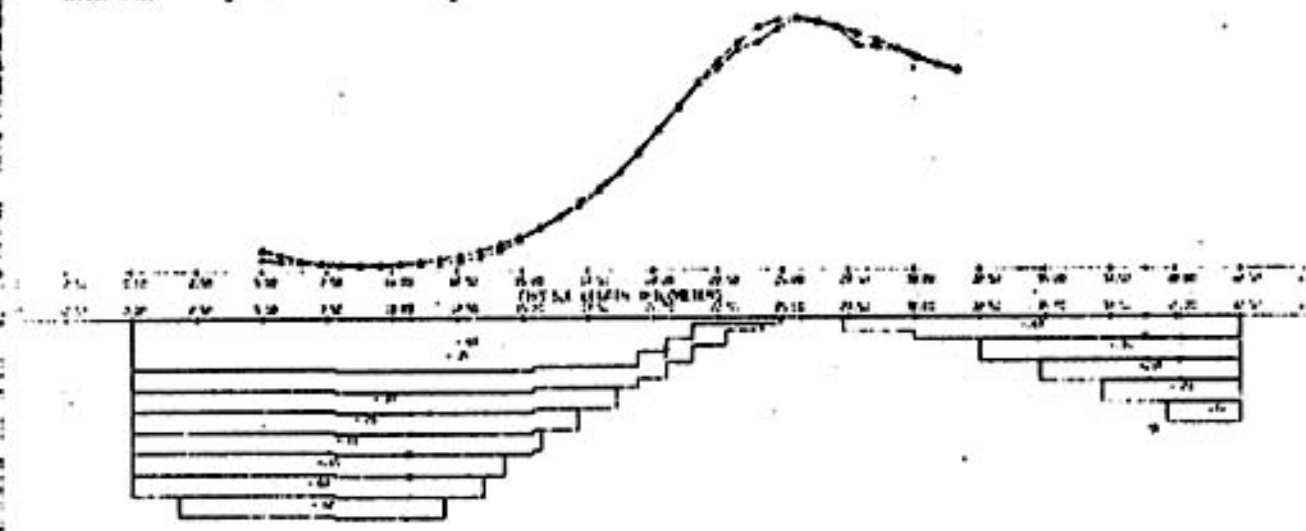
TABLE II. OBSERVED AND COMPUTED GRAVITY ANOMALIES.

profile 4A'		profile 43'	
observed anomalies	computed anomalies	observed anomalies	computed anomalies
-5.50	-5.54230	-28.5	-29.6535
-4.60	-4.44265	-29.2	-29.8906
-4.20	-3.65408	-29.7	-30.0654
-3.30	-2.72641	-30.0	-30.2049
-2.70	-2.23905	-30.2	-30.3211
-2.00	-1.81746	-30.4	-30.3650
-1.40	-1.45569	-30.4	-30.3197
-1.10	-1.46845	-30.3	-30.1895
-0.60	-0.85184	-30.2	-29.9690
-1.10	-0.83396	-30.1	-29.6491
-2.00	-2.57292	-29.9	-29.2204
-3.40	-3.07934	-29.4	-28.6689
-4.80	-5.26611	-28.6	-27.9745
-6.40	-7.18420	-27.4	-27.1085
-8.50	-8.59209	-26.0	-26.0460
-10.1	-10.6716	-24.7	-24.8405
-11.2	-12.0104	-23.0	-23.4477
-12.6	-13.3823	-21.4	-21.8192
-13.5	-14.4074	-19.5	-19.7799
-14.7	-15.2395	-17.5	-17.1594
-15.8	-16.0733	-14.6	-14.6474
-16.9	-16.9788	-11.9	-12.1653
-17.6	-18.1494	-9.10	-9.35359
-18.8	-19.7330	-6.70	-7.52665
-19.9	-20.5127	-4.50	-5.33539
-20.9	-20.9932	-2.70	-4.40232
-21.4	-21.2829	-1.90	-2.90028
-21.3	-21.4198	-1.60	-1.60454
-20.7	-21.4253	-2.00	-2.23088
		-2.70	-2.73750
		-3.50	-4.91583
		-4.30	-5.11572
		-5.20	-5.34413
		-6.20	-6.47330
		-7.10	-7.14410
		-8.00	-7.63903

FIGURE 1. PROFILE OF THE DAM AND THE DAM FOUNDATION AT THE DAM SITE.  
 (A) DAM PROFILE IN SECTION OF ST. LAWRENCE DAM, ST. LAWRENCE DAM, Q.E.  
 (B) DAM FOUNDATION  
 (C) DAM FOUNDATION



FORCE, THE ORIGINAL SMOOTHED AND THE RESULT OF WORKER BASE IN  
 WHICH CASE IS THE CASE OF REALTIME WITH DATA, YEAR DISTANCE  
 MODEL NAME: B  
 MODEL NAME: B



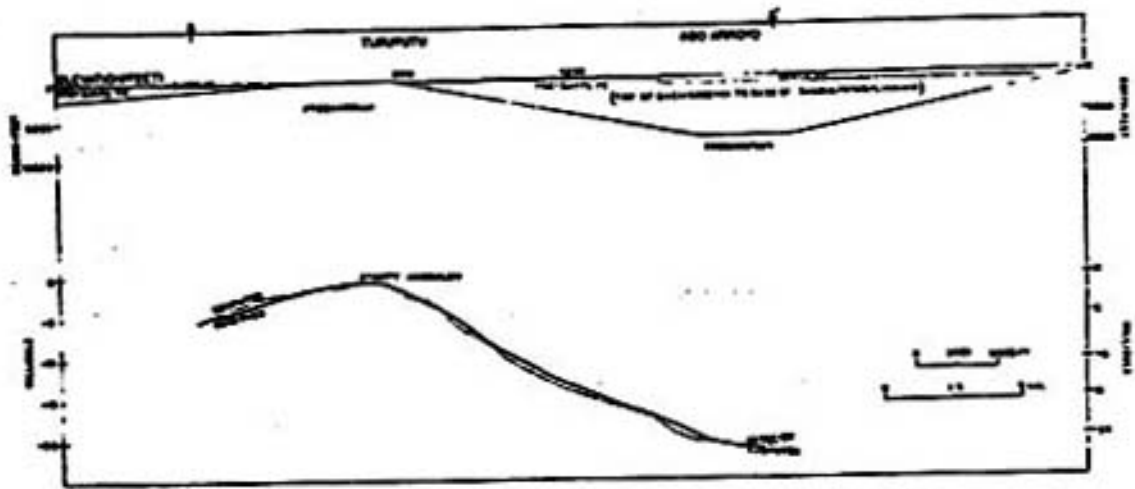
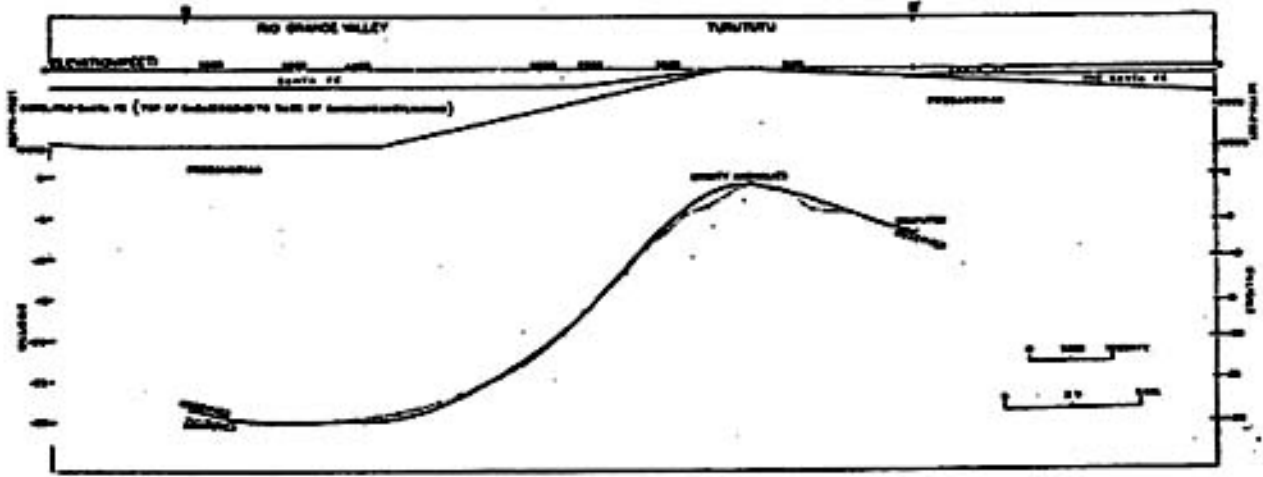


FIGURE 1. ELEVATION, SECTION, AND PROFILE OF THE DAM AND DAM FOUNDATION



shallower until at Turututu, Precambrian rocks are exposed or in the matter of fact, this Precambrian rocks are overlaid by the thin thickness of basalt. The model of profile AA' shows that the depth to Precambrian basement rocks is about 7500 feet at north-eastern area of residual Bouguer anomalies map, near Jansano mountains.



## SUMMARY AND CONCLUSIONS

This gravity survey is covered the area about 240 square miles. The 88 gravity stations were occupied by using Worden gravity meter. Residual Bouguer anomalies map shows Rio Grande depression and the other depression near Manzano mountains. The faults are shown on the west of Los Pinos mountains and on the north-western area of the map. The computed gravity anomalies and observed gravity anomalies are matched both of the profile AA' and profile BB'. The thickness of Custerian and Santa Fe formation in Rio Grande valley is 2130 feet by the calculation, and 2500 feet by the computation; while in the depression near Manzano mountains is 797 feet by the calculation, and 950 feet by the computation.

## APPENDIX I

### THE GRADIENT OF THEORETICAL GRAVITY VALUES

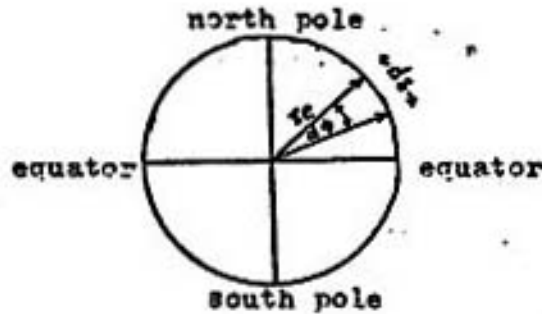


Figure 16. Diagram for the gradient of theoretical gravity values.

The value of the gradient of  $g_{th}$  of each reference latitude is  $\frac{d g_{th}}{d s}$ . The varied distance  $d s$  along the meridian of the earth will make the angle of the latitude changes to  $d\phi$ . The average radius of the earth is  $r_e$ .

$$\text{From, } g_{th} = g_e ( 1 + C_1 \sin^2 \phi - C_2 \sin^2 2\phi )$$

$$\text{and, } d s = r_e d\phi$$

$$\begin{aligned} \text{Therefore, } \frac{d g_{th}}{d s} &= \frac{g_e}{r_e} ( 2 C_1 \sin \phi \cos \phi - 4 C_2 \sin 2\phi \cos 2\phi ) \\ &= \frac{g_e}{r_e} ( C_1 \sin 2\phi - 2 C_2 \sin 4\phi ) \end{aligned}$$

$$\text{where, } g_e = 978.04900 \text{ gals,} \quad C_1 = 0.005288384,$$

$$r_e = 6371.221 \times 10^5 \text{ cm,} \quad C_2 = 0.000005869,$$

$$\text{Hence, } \frac{d g_{th}}{d s} = 24.6 \times 10^{-5} \text{ milligal/feet } \sin 2\phi$$

## APPENDIX II

### THE VERTICAL ATTRACTION OF GRAVITY OF AN INFINITE PLATE

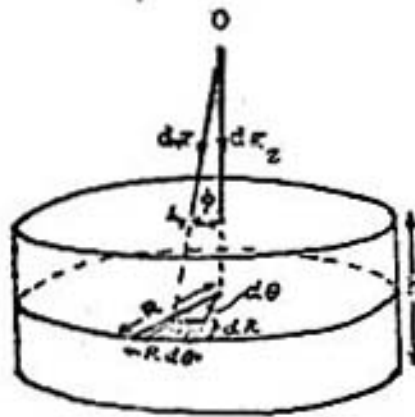


Figure 17. Diagram Illustrating Bouguer plate Correction.

From Fig. 17,

$h$  is the height of the plate,

$R$  is the radius of the plate extend to infinity.

$\rho$  is the volume density of the plate = mass/volume.

$\sigma$  is the surface density of the plate = mass/area.

$g_z$  is the vertical attraction of gravity along the  $Z$  axis.

Consider the small area  $dA$  in the plate, which is the distance  $r$  from the gravity observation station  $O$ , and this direction makes the angle  $\phi$  with the  $Z$  axis. That small area  $dA$  has the small angle  $d\theta$  from the center of the plate.  $M$  is the mass of the plate.

$$dz = \frac{G M}{r^2} = \frac{G \sigma dA}{r^2} = \frac{G \sigma R d\theta dR}{r^2}$$

because,  $dA = R d\theta dR$

but,  $dg_z = dg \cos \phi = \frac{dg z}{r}$

therefore,  $g_z = \frac{G \sigma z R dR d\theta}{(R^2 + z^2)^{3/2}}$

$$\begin{aligned}
 g_z &= G \sigma z \int_0^{2\pi} \int_0^R \frac{R dR d\theta}{(R^2 + z^2)^{3/2}} \\
 &= 2\pi G \sigma z \left[ \frac{-1}{(R^2 + z^2)^{1/2}} \right]_0^R \\
 &= 2\pi G \sigma z \left[ \frac{1}{z} - \frac{1}{(R^2 + z^2)^{1/2}} \right]
 \end{aligned}$$

If R is extend to infinity,

$$\frac{1}{(R^2 + z^2)^{1/2}} = 0$$

Therefore,  $g_z = 2\pi G \sigma = 2\pi G \rho h.$

APPENDIX III

DRIFT CORRECTION

TABLE III

station	time	reading scale divisions	drift corrections	reading after drift correctio
S15	14.14	473.80	0	473.80
S16	14.23	529.10	-0.06	539.04
S17	14.28	528.70	-0.09	528.61
S19	14.37	560.70	-0.14	560.56
S20	14.43	532.50	-0.19	532.31
S21	14.49	494.40	-0.23	494.17
S15	15.00	474.10	-0.30	473.80

From the Table III, between the two readings of the base station S15, the difference values from the two readings is plotted against the time, as shown in figure 18. The reading after drift correction can be calculated. The reading gravity value at each station in milligal can be determined by the multiplication of the instrument constant with the reading gravity value in scale division after drift correction.

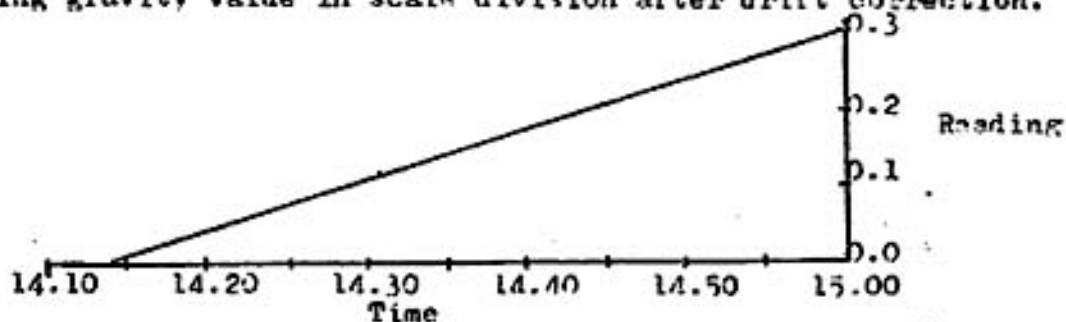


Figure 18. The diagram of drift correction.

APPENDIX IV

DETERMINATION THE DEPTH OF TWO DIMENSIONAL VERTICAL FAULT

Consider the formula,

$$g_z = 2 G \Delta \rho t \left[ \frac{\pi}{2} - \tan^{-1} \frac{X}{Z} \right]$$

where,  $g_z$  is the vertical attraction of the gravity along the Z axis,

$\Delta \rho$  is the density contrast of the formation lower and upper the fault,

t is the different thickness of the lower bed and upper bed of the fault,

Z is the depth to the center of the different thickness of the lower bed and upper bed of the fault,

X is the gravity station.

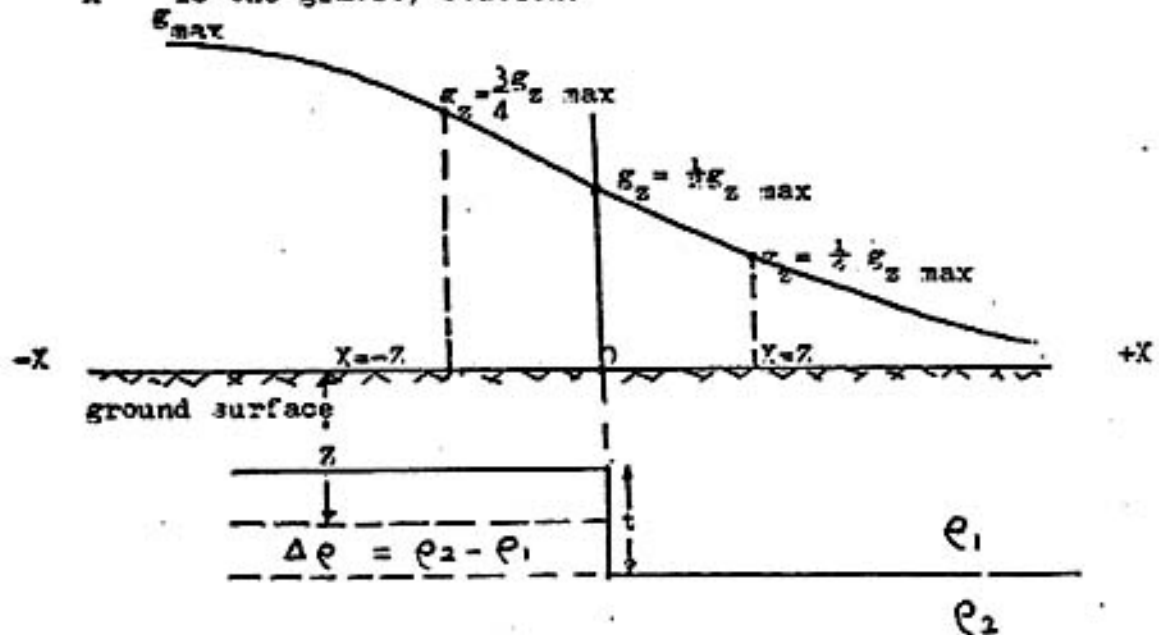


Figure 19. Gravity profile above the two dimension vertical fault.

When,  $X=0$ ,  $\epsilon_z = \pi G \Delta \rho t$

$X=Z$ ,  $\epsilon_z = \frac{\pi G}{2} \Delta \rho t$

$X=-Z$ ,  $\epsilon_z = \frac{3}{2} \pi G \Delta \rho t$

$X=\infty$ ,  $\epsilon_z = 0$

$X=-\infty$ ,  $\epsilon_z = 2 \pi G \Delta \rho t = \epsilon_z \text{ maximum.}$

Therefore, when  $X=0$ ,  $\epsilon_z = \frac{1}{2} \epsilon_z \text{ maximum.}$

From the gravity profile, the value of  $\epsilon_z = \frac{1}{2} \epsilon_z \text{ maximum}$  can be determined and the position of the edge of the fault is known.

The depth  $Z$  can be found by the value of  $\epsilon_z = \frac{3}{4} \epsilon_z \text{ maximum}$  ( $X=-Z$ ),

or  $\epsilon_z = \frac{1}{4} \epsilon_z \text{ maximum}$  ( $X=Z$ ).

## APPENDIX V

### GEOLOGIC CORRECTIONS

When a gravity station is near Precambrian rocks, but is not on Precambrian rocks. The regional Bouguer anomalies must be the anomalies that the gravity stations are on Precambrian rocks. So, the geologic corrections must be used. If a gravity station is lied on the rocks that overly on Precambrian rocks about 5000 feet. From the geologic section of figure 10, the density contrast between the density of each section with the density of Precambrian rocks, from Sandia formation up to 5000 feet can be determined. The average of the density contrast of the rocks of 5000 feet thick, can obtained.

1. The density contrast of Sandia formation of thickness 1000 feet is,

$$2.667 - 2.55 = 0.117 \text{ gram/cm}^3.$$

2. The density contrast of Wadera formation of thickness 1000 feet is,

$$2.667 - 2.6 = 0.067 \text{ gram/cm}^3.$$

3. The density contrast of Bursum, Abo, and Yeso formation of thickness

$$1000 \text{ feet is, } 2.667 - 2.52 = 0.147 \text{ gram/cm}^3.$$

4. The density contrast of Yeso, and San Andres formation of thickness

$$1000 \text{ feet is, } 2.667 - 2.56 = 0.107 \text{ gram/cm}^3.$$

5. The density contrast of Dockum, Dakota, and Mancos formation of

$$\text{thickness 1000 feet is, } 2.667 - 2.38 = 0.287 \text{ gram/cm}^3.$$

The average of these density contrast is,

$$\frac{0.117 + 0.067 + 0.147 + 0.107 + 0.287}{5} = 0.145 \text{ gram/cm}^3.$$



$$g = 2 \pi \rho G h = 0.01276 \rho h \text{ milligal.}$$

$$g = 0.01276 \times 0.145 \times 5000 = 9.25 \text{ milligals.}$$

The geologic correction for this gravity station is 9.25 milligals.

This correction is directly subtracted from the Bouger gravity anomaly.

meter Observations", *Geophysics*, V. 4, n. 176.

11. Sanford, A.R.. 1968, "Gravity Survey in Central Socorro County, New Mexico". State Bureau of Mines and Mineral Resources, New Mexico Institute of Mining and Technology, Socorro, New Mexico. Circular 91.

12. Stark, J.T., and Dapples, E.C., 1946, "Geology of the Los Pinos Mountains, New Mexico", *Geol. Soc. American Bull.*, V. 57.

13. Talwani, M., J.L. Worzel, and A. Landisman, 1959, "Rapid Gravity Computations for Two Dimensional Bodies with Application to the Mendocino Submarine Fracture Zone", *Geophysical Res. Vol. 64, No. 1*, n. 49-59.

14. Wilpolt, R.H., et al., 1946, "Geologic Map and Stratigraphic of Paleozoic Rocks of Joyita Hills, Los Pinos Mountains and Northern Chusadera Mesa, Valencia, Torrence, and Socorro Counties, New Mexico". U.S. Geol. Survey Oil and Gas Inv. Prelim. Map 61.